

# Overcoming the Instability of Gaseous Peptide Phosphate Ester Groups by Dimetal Protection\*\*

Simon Svane, Fedor Kryuchkov, Anders Lennartson, Christine J. McKenzie, and Frank Kjeldsen\*

Phosphorylation is the most prolific type of post-translational modification in proteins and is involved in many important biological processes such as signal transduction, cell division, gene expression, cytoskeletal regulation, and metabolic maintenance.<sup>[1]</sup> The biological importance of protein phosphorylation has driven efforts towards the discovery of reliable analytical techniques for the sequencing and analysis of phosphorylated sites. The typical approach involves tryptic protein digestion and subsequent sequencing by tandem mass spectrometry (MS/MS) using vibrational excitation (VE) of the gas-phase phosphopeptide ions. The most widely used technique for VE is collision-activated dissociation (CAD). Whereas sequencing of nonmodified peptide ions with CAD MS/MS is becoming routine, phosphopeptide analysis remains a challenge. The predominant reason for this is the significant instability of the phosphate ester bond in VE of phosphopeptide ions.<sup>[2,3]</sup> This instability can be rationalized by a comparison of the activation barriers for cleavage of the amide bonds (ca. 40 kcal mol<sup>-1</sup>)<sup>[4]</sup> versus that of the phosphate ester bond (< 20 kcal mol<sup>-1</sup>).<sup>[5]</sup> Thus, the phosphate ester groups are prone to facile detachment (e.g. as H<sub>3</sub>PO<sub>4</sub>) from phosphorylated peptide ions, and reliable determination of the phosphorylation site is hence complicated.<sup>[3]</sup> Electron capture dissociation (ECD)<sup>[6]</sup> and electron transfer dissociation (ETD)<sup>[7]</sup> are capable of producing sequence-specific backbone cleavages without such extensive detachment of labile modifications;<sup>[8]</sup> however, these techniques have not yet become the method of choice in large-scale phosphopeptide analysis.

The strategy we have explored to circumvent the limitations of the current MS/MS fragmentation approach is to chemically inhibit detachment of the phosphate group during VE. Our hypothesis was that the affinity of the oxoanion motif of the phosphate ester group towards certain dimetallic sites in metalloenzymes and coordination complexes could be tuned for gas-phase applications in phosphoproteomics. Dimetallic complexes of a septadentate phenolato-hinged

acyclic dinucleating ligand that contains auxiliary, water-derived ligands<sup>[9,10]</sup> or phosphate-ester bridging groups,<sup>[11,12]</sup> have been structurally characterized, and these compounds model both our envisaged starting and product motifs. Herein we present evidence for an increased stabilization of phosphate ester bonds in phosphorylated peptide ions during CAD MS/MS achieved by the complexation of their phosphate ester motif by the pentacationic “dimetallic tag” [Ga<sub>2</sub>(bpbp)]<sup>5+</sup> (**1**; Ga<sub>2</sub>C<sub>36</sub>H<sub>39</sub>N<sub>6</sub>O; *M*<sub>mono</sub> = 709.1697 Da; Hbpbp = 2,6-bis((*N,N'*-bis(2-picolyl)amino)methyl)-4-*tert*-butylphenol), which is generated in situ during the anation reaction of the precursor [Ga<sub>2</sub>(bpbp)(OH)<sub>2</sub>(OH<sub>2</sub>)<sub>2</sub>]<sup>3+</sup> (**2**) by a phosphorylated peptide in aqueous solution [Eq. (1)]. We coin this methodology “dimetal phosphate ester stabilization” (DIMPES).



The formulation of the solution state of precursor **2** is supported by the analysis of the solid state. [Ga<sub>2</sub>(bpbp)(OH)<sub>2</sub>(OH<sub>2</sub>)<sub>2</sub>](ClO<sub>4</sub>)<sub>3</sub> (**2**(ClO<sub>4</sub>)<sub>3</sub>), was characterized by single-crystal X-ray diffraction (Figure 1). This complex is in fact one of only a handful of structurally characterized complexes containing the potentially reactive pseudo-bridging (O<sub>2</sub>H<sub>3</sub>)<sup>-</sup> motif.<sup>[13–15]</sup>

Figure 2 shows the mass spectra of the native untagged and **1**-tagged phosphopeptide FQpSEEQQTEDELQDK. The spectrum of the untagged phosphopeptide is dominated by doubly protonated ions [*M*+2H]<sup>2+</sup> (Figure 2a). Reaction

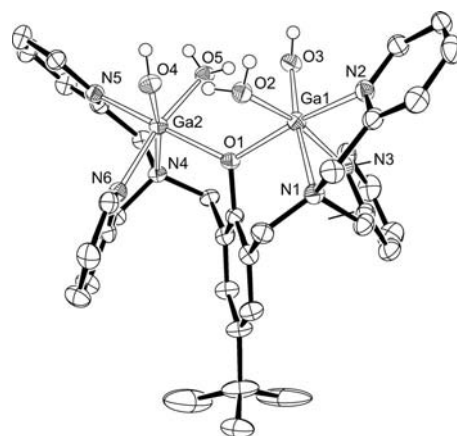


**Figure 1.** The X-ray crystal structure of **2**. The Ga...Ga distance is 3.641(8) Å and the O...O distances for the auxiliary H-bonded water and hydroxide ligands bound to adjacent gallium ions are 2.488(8) Å (O2...O4) and 2.491(8) Å (O3...O5).

[\*] F. Kryuchkov, Prof. F. Kjeldsen  
Department of Biochemistry and Molecular Biology  
Campusvej 55, 5230 Odense M (Denmark)  
E-mail: frankk@bmb.sdu.dk

S. Svane, Dr. A. Lennartson, Prof. C. J. McKenzie  
Department of Physics, Chemistry and Pharmacy  
Campusvej 55, 5230 Odense M (Denmark)

[\*\*] This work was supported by the Danish Council for Independent Research, Natural Sciences (FNU grant FK272-08-0044 to FK).

Supporting information for this article is available on the WWW under <http://dx.doi.org/10.1002/anie.201108481>.

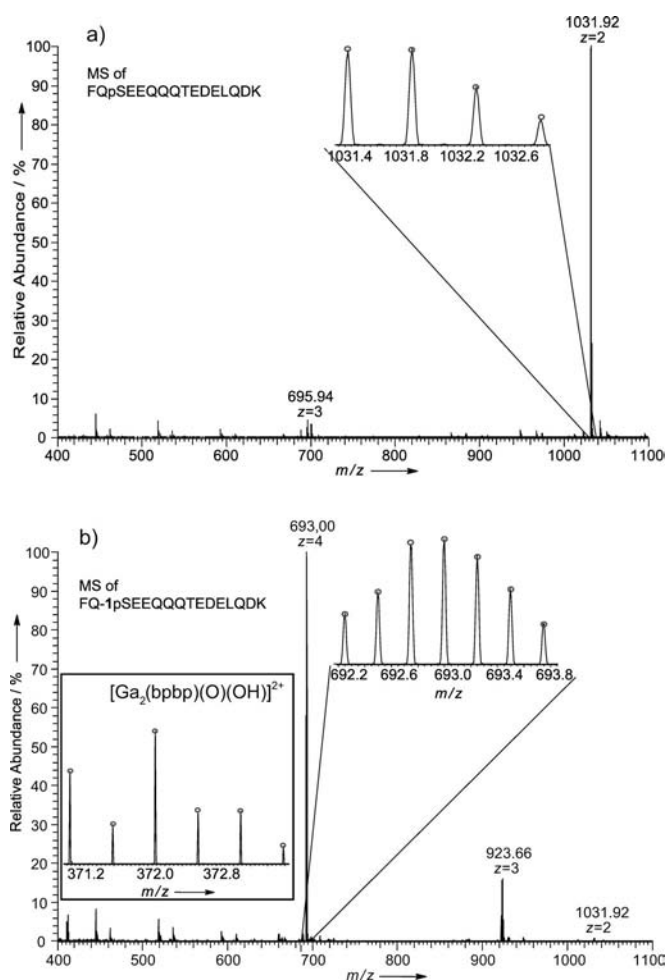


**Figure 2.** a) Mass spectrum of FQpSEEQQQTEDELQDK with the signals of the doubly charged precursor ions at  $m/z$  1032 enlarged and b) mass spectrum of 1-tagged FQ-1pSEEQQQTEDELQDK with the signals of the quadruply charged precursor ions at  $m/z$  693 enlarged and the isotope distribution of [Ga<sub>2</sub>(bpbp)(O)(OH)]<sup>2+</sup> (Ga<sub>2</sub>C<sub>36</sub>H<sub>40</sub>N<sub>6</sub>O<sub>3</sub>,  $M_{\text{mono}} = 742.1674$  Da) shown in the inset on the left.

of precursor 2 with the phosphopeptide in solution and subsequent MS gives the spectrum shown in Figure 2b. Efficient tagging is evident by the abundance of the ion signals at  $m/z$  692.2476 [ $M+1-H$ ]<sup>4+</sup> and  $m/z$  922.6608 [ $M+1-2H$ ]<sup>3+</sup>. The tagged phosphopeptide ions have the generic formula [ $M+n1-n2H+mH$ ]<sup>(3n+m)+</sup>, which was confirmed by accurate mass measurements (mass deviation was 2.4 ppm) as well as by high correlation between the experimental and the theoretical isotopic envelope shown in the inset of Figure 2b.

The tagged ions display a characteristic atypical peptide isotopic pattern that has previously been argued to hold analytical potential for recognition of phosphorylated peptides.<sup>[16]</sup> Another advantage of the DIMPES approach is the significant increase in the charge state of the tagged phosphopeptides from 2+ to 4+. Greater charge state translates into proportionally greater signal abundance in mass spectrometers with image current detection, such as the popular orbitrap MS.

The remarkable specificity of tag 1 was evaluated using a mixture of tryptic peptides of 12 proteins of which three were phosphorylated ( $\alpha$  casein,  $\beta$  casein and ovalbumin). This sample was analyzed by CAD LC-MS/MS. A full-scan MS spectrum with both phosphorylated and nonphosphorylated peptides co-eluting from the analytical column is shown in Figure 3a. Only the phosphorylated peptide FQpSEEQQQTEDELQDK was tagged with 1 in the presence of at least

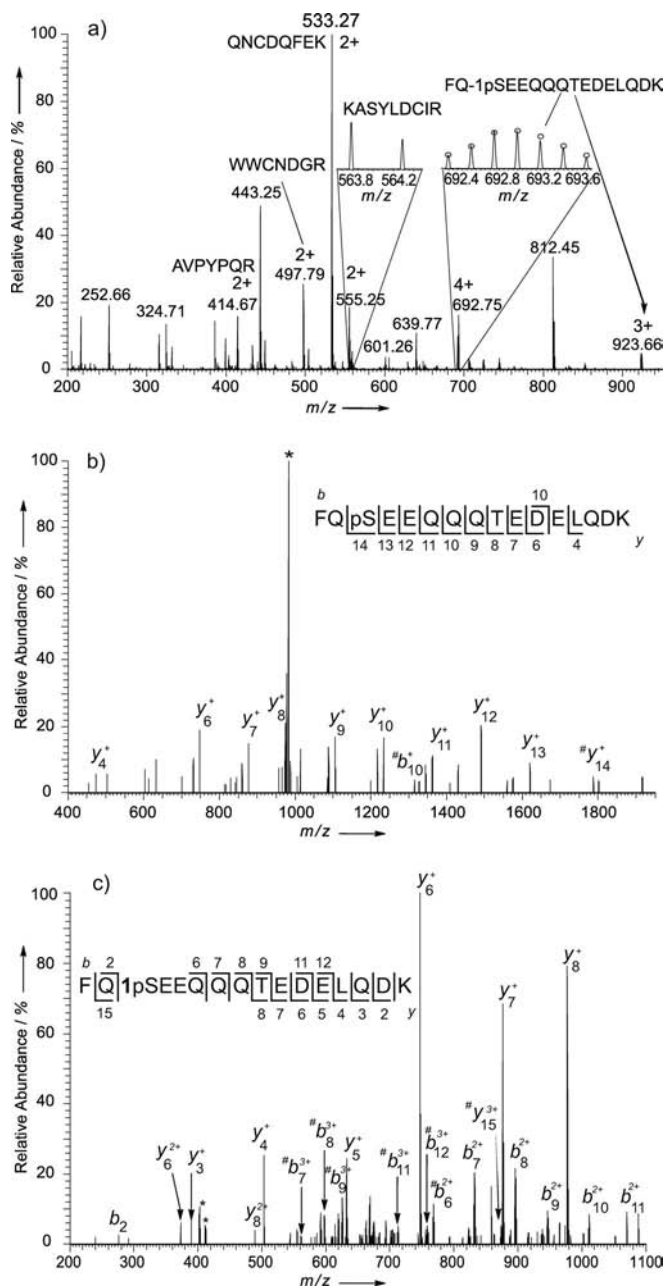


**Figure 3.** a) LC-MS/MS of [FQ-1pSEEQQQTEDELQDK-H]<sup>4+</sup> co-eluting with four nonphosphorylated peptides with the peaks of  $m/z$  564 and  $m/z$  693 enlarged, b) CAD of [FQpSEEQQQTEDELQDK+2H]<sup>2+</sup> and c) CAD of [FQ-1pSEEQQQTEDELQDK-H]<sup>4+</sup>. In (b) and (c), the  $y$ -fragment (C-terminal fragments) and the  $b$ -fragment series (N-terminal fragments) are indicated by the numbers below and above the peptide sequence, respectively. Loss of a phosphate group is depicted with asterisk. Phosphate-containing fragments are marked with #.

four other nonphosphorylated peptide ions (Figure 3a). Similarly, no observation of unspecific attachment of tag **1** was found among 30 other randomly chosen nonphosphorylated peptides (Table S3 in the Supporting Information).

CAD MS/MS spectra of FQpSEEQQQTEDELQDK and its tagged derivative FQ-1pSEEQQQTEDELQDK are shown in Figure 3b,c. As expected, the prominent fragment of the native phosphopeptide was that of  $\text{H}_3\text{PO}_4$  loss (24 % of the total product ion yield). By comparison, the **1**-tagged phosphopeptide lost the phosphate group only as minor fragmentation channels (3.5 %). These losses are observed as  $[(\text{Ga}_2(\text{bpbp})(\text{PO}_4))^{2+}]$  at  $m/z$  402.061 and  $[(\text{Ga}_2(\text{bpbp})(\text{PO}_4\text{H})(\text{OH}))^{2+}]$  (or  $[(\text{Ga}_2(\text{bpbp})(\text{PO}_4)(\text{H}_2\text{O}))^{2+}]$  at  $m/z$  411.066. The significant reduction in phosphate ester bond cleavage when protected by tag **1** suggests an increased bond stability of this functional group. As a result, in **1**-tagged phosphopeptide ions, the backbone amide bonds, which will produce sequence-specific fragment ions when broken, are now more labile than the phosphate ester bond.

We then investigated if these findings are generally applicable for other phosphopeptides by using a phosphopeptide-enriched sample of  $\alpha$  and  $\beta$  casein. Table 1 summarizes the results of CAD LC-MS/MS of eight phosphopeptides with and without tagging by **1**.

Generally, the average charge state increased by almost a factor of two for all tagged phosphopeptides. In all cases, but one, the sequence coverage of the tagged phosphopeptides was found to be larger or equivalent to the nontagged

phosphopeptides. Notably, the phosphate detachment from native phosphopeptides varied from 6.2–100 % (average 38.9 %), whereas it varied only from 0–8.6 % (average 4.4 %) for **1**-tagged phosphopeptides. Furthermore,  $\text{H}_3\text{PO}_4$  loss was observed only from fragment ions of native phosphopeptides. Based on these experimental results we give the following explanation for the strengthening of the phosphate ester bond. While the geometry of tag **1** dictates the specificity towards the phosphate group, we propose that the large positive charge of **1** is responsible for its stabilization. The charge status of the phosphate ester group is deduced from the MS/MS data to be doubly deprotonated when bound to **1**. This charge status suggests that loss of the phosphate ester group from **1**-tagged phosphopeptides under VE conditions should be considered in relation to the commonly accepted fragmentation pathway for deprotonated phosphopeptides in the negative ion mode (Scheme 1, top). In the latter the phosphate ester group can, upon VE, overcome the barrier for dislocation of a lone pair with subsequent P–O bond cleavage.<sup>[17,18]</sup> We suggest that the large excess of positive charge of tag **1** (overall 5+) when bound to the phosphate ester is inducing substantial charge transfer from the doubly deprotonated phosphate group to the Ga atoms of **1**. This suggestion is supported by recent DFT calculations of a similar dinuclear vanadium complex.<sup>[19]</sup> In that study, the sum of the Mulliken charges on  $\text{HPO}_3^{2-}$  was reduced from –1 (free anion) to –0.356 upon complex formation with the 3+ vanadium complex  $[(\text{VO})_2(\text{bpbp})]^{3+}$ . An even larger reduction in the electron density of the phosphate ester is expected when it is attached to **1** since the charge of **1** is 70 % larger than that of the vanadium complex.

The resulting substantial loss of negative charge on the phosphate ester group precludes the otherwise dominating fragmentation channel initiated by the free lone pair (Scheme 1, middle). This is consistent with the absence of  $[(\text{Ga}_2(\text{bpbp})(\text{PO}_3))^{4+}]$  in CAD MS/MS. This hypothesis correlates with the fact that the only phosphate loss observed in CAD MS/MS was as  $[(\text{Ga}_2(\text{bpbp})(\text{PO}_4))^{2+}]$  and its hydrated adduct at  $m/z$  402.0631 and  $m/z$  411.0685, respectively. These losses involve cleavage of the C–O bond and its suggested mechanism is depicted in Scheme 1, bottom.

In conclusion, we have demonstrated that highly specific tagging with a specifically designed dinuclear gallium complex can increase the stability of the peptide phosphate ester bond. This methodology allows for the sequencing of phosphopeptides using CAD while

**Table 1:** CAD LC-MS/MS of **1**-tagged and native phosphopeptide ions in different charge states.

Peptide sequence	Precursor charge state [+]	Sequence coverage [%] <sup>[a]</sup>	Phosphate loss [%] <sup>[b]</sup>	Precursor phosphate loss [Y/N] <sup>[c]</sup>	Fragment phosphate loss [Y/N] <sup>[c]</sup>	Determination of phosphosite [Y/N] <sup>[c]</sup>
FQ-1pSEEQQQTEDELQDK	3	67	0.0	Y	N	Y
FQ-1pSEEQQQTEDELQDK	4	87	2.7	Y	N	Y
FQpSEEQQQTEDELQDK	2	66	28.0	Y	Y	Y
YKVPQLEIVPN-1pSAEER	4	40	0.0	N	N	Y
YKVPQLEIVPN-1pSAEER	5	46	2.9	Y	N	Y
YKVPQLEIVPNpSAEER	2	13	37.0	Y	Y	Y
YKVPQLEIVPNpSAEER	3	46	6.2	Y	Y	Y
EQLST-1pSEENSK	3	70	7.7	Y	N	N
EQLST-1pSEENSK	4	40	7.3	Y	N	N
EQLSTpSEENSK	2	60	23.7	Y	Y	Y
VNEL-1pSK	3	80	6.4	Y	N	Y
VNELpSK	2	40	44.9	Y	Y	Y
VPQLEIVPN-1pSAEER	3	65	1.3	Y	N	Y
VPQLEIVPN-1pSAEER	4	71	4.9	Y	N	Y
VPQLEIVPNpSAEER	2	38	25.1	Y	Y	Y
NMAINP-1pSK	3	43	3.8	Y	N	Y
NMAINPpSK	2	57	37.2	Y	N	Y
EKVNEL-1pSK	3	70	8.6	Y	N	Y
EKVNELpSK	2	0	47.9	Y	N/A	N
EQLST-1pSEENSKK	3	64	5.6	Y	N	Y
EQLST-1pSEENSKK	4	36	6.6	Y	N	N
EQLSTpSEENSKK	2	0	100.0	Y	N/A	N

[a] Ratio of the number of backbone cleavages compared to the theoretically possible number.

[b] Summed abundance of phosphate loss from precursor and fragment ions as percentage of total ion abundance in the spectrum (200 most abundant ion signals). [c] Y = yes, N = no, N/A = not applicable.

